

Optical and dielectric properties of ZnO tetrapod structures at terahertz frequencies

Jianguang Han and Zhiyuan Zhu

Shanghai Institute of Applied Physics, Chinese Academy of Sciences, Shanghai 201800, People's Republic of China

Sanith Ray, Abul K. Azad, and Weili Zhang^{a)}

School of Electrical and Computer Engineering, Oklahoma State University, Stillwater, Oklahoma 74078

Mingxia He

School of Electrical and Computer Engineering, Oklahoma State University, Stillwater, Oklahoma 74078 and College of Precision Instrument and Optoelectronics Engineering, Tianjin University, Tianjin 300072, People's Republic of China

Shihong Li and Yiping Zhao

Nanoscale Science and Engineering Center, Department of Physics and Astronomy, University of Georgia, Athens, Georgia 30602

(Received 25 February 2006; accepted 24 May 2006; published online 18 July 2006)

The low-frequency optical and dielectric properties of ZnO tetrapod structures prepared by thermophysical method were studied by terahertz time-domain spectroscopy. The power absorption, refractive index, and the complex dielectric function were measured in the frequency range from 0.2 to 3.5 THz. Based on a simple effective medium theory, the low-frequency dielectric properties of ZnO tetrapods were found to be associated with the transverse optical E_1 phonon mode, which is consistent with that observed in bulk single-crystal ZnO. © 2006 American Institute of Physics. [DOI: 10.1063/1.2222329]

Zinc oxide (ZnO) is an excellent II-VI compound semiconductor for low-voltage and short-wavelength optoelectronics applications because of a direct wide band gap of 3.37 eV, high exciton gain, and a large exciton binding energy of ~ 60 meV.^{1,2} The minimum fabrication barrier, rather high mobility (~ 200 cm²/Vs) and high resistivity also enable the single-crystal ZnO to be an ideal choice for high power terahertz generation.³ ZnO nanostructures are reported to have potential applications for piezoelectric transduction, optical emission, catalysis, actuation, drug delivery, and optical storage with promising photoelectronic, photochemical, and catalytic properties.⁴ The increase in surface area and the quantum confinement effects have made nanostructured materials quite distinct from their bulk form in both electrical and optical properties. Various one-dimensional structures of ZnO, such as tetrapods, nanowires, and nanobelts, have attracted much attention.⁵ In particular, the ZnO tetrapod structures are expected to exhibit some special properties because of their single crystalline structure and controllable morphology.⁶ The ZnO tetrapods are reported to have good responses to ethanol and methane at different levels and temperatures, which make them a good choice for gas sensors.⁷ The Mn-doped ZnO tetrapod structures were found to be ferromagnetic with Curie temperature ~ 50 K and showed a large coercive field, thus allowing electromagnetic and spintronics applications. This helps combine microelectronics and nanoelectronics with spin-dependent effects for the next generation devices.⁸

Recently, ZnO tetrapods have shown intriguing lasing properties by having diameter of the arms comparable to excitation wavelength.^{9,10} Spectroscopic study of ZnO tetrapods is necessary to characterize their optical properties over a broad frequency range and to further explore their potential

applications in broad areas. In this letter, we present a study of far-infrared spectroscopic properties of ZnO tetrapods in the frequency range from 0.2 to 3.5 THz (1.5 mm–86 μ m) by using terahertz time-domain spectroscopy (THz-TDS), a preferably recognized far-infrared spectroscopic approach due to high signal-to-noise ratio ($>10\,000:1$), coherent phase information, and nonionizing properties.¹¹ The dielectric and optical properties of ZnO tetrapods were extrapolated using a simple effective medium theory.^{12,13} The THz-TDS system utilized to characterize the ZnO tetrapod structures was a photoconductive switch-based spectrometer and has a frequency-independent beam waist of 3.5 mm as described previously.¹⁴

The ZnO tetrapods were grown by the vapor phase transport methods by heating the Zn powder to 700 °C in a quartz tube furnace at ambient pressure and with the flow of argon gas.¹⁰ The individual tetrapod samples were isolated by sonicating them in methanol. Scanning electron microscope (SEM) and optical microscope were used to characterize the shape and the size of the tetrapods, and x-ray diffraction revealed the hexagonal wurtzite structures. The diameter of the legs was estimated to be between 200 and 800 nm, while the length of the legs was between 10 and 30 μ m.^{15,16} The SEM images of a bundle of ZnO tetrapods are shown in Fig. 1. The ZnO tetrapod samples for analysis were placed in a cell made of two 10.9×11.0 mm² windows and a 1.288 mm spacer. Both the windows and the spacer were made from *p*-type silicon wafer with thickness of 640 μ m and resistivity of 20 Ω cm. An identical empty cell was used as a reference. Both cells were placed in an aluminum holder and centered over a 5-mm-diameter hole to define the optical aperture.

The transmitted terahertz pulses through both the reference and the ZnO tetrapod sample were measured. A relatively clean separation in time between the main transmitted sample pulse and the first reflection enables the data analysis

^{a)}Electronic mail: wwzhang@okstate.edu

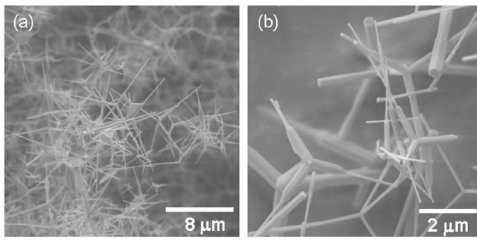


FIG. 1. The SEM images of ZnO tetrapods with leg diameters of 200–800 nm and lengths of 10–30 μm : (a) ZnO tetrapod bundle; (b) magnified image.

on the main pulse only.¹⁴ The sample and the reference pulses were Fourier transformed to obtain the corresponding complex amplitude spectra. To extrapolate the power absorption and refractive index, the ratio between the spectra of the reference and the sample gave the effective absorption by the sample, whereas the phase shift was calculated to determine the refractive index.¹⁷ The frequency dependent power absorption coefficient $\alpha(\omega)$ and the refractive index $n(\omega)$ are plotted as open circles in Fig. 2. The measured power absorption increases as a function of frequency and no prominent absorption peak is observed below 3.5 THz, whereas the refractive index approaches nearly a constant of 1.03.

The frequency-dependent dielectric response $\varepsilon(\omega)$ is described by the relationship, $\varepsilon(\omega) = \varepsilon_r(\omega) + i\varepsilon_i(\omega) = [n(\omega) + ik(\omega)]^2$, where the imaginary part of the refractive index k is related to the power absorption as $k(\omega) = \alpha(\omega)\lambda_0/4\pi$,¹⁴ and $\varepsilon_r(\omega)$ and $\varepsilon_i(\omega)$ are the real and imaginary parts of the dielectric function. The open circles in Figs. 3(a) and 3(b) illustrate the measured complex dielectric constant of the ZnO tetrapods extracted from the data of power absorption and refractive index. Since the sample to be measured is loosely packed ZnO tetrapods and consists of both ZnO tetrapods and air, the dielectric constant plotted in Fig. 3 is the effective complex dielectric constant ε_{eff} , with the contributions from both the air and the pure ZnO tetrapods. A simple effective medium theory (EMT) was employed to obtain the effective dielectric function of ZnO tetrapods,^{12,13} $\varepsilon_{\text{eff}}(\omega) = f\varepsilon_m(\omega) + (1-f)\varepsilon_h$, where the filling factor f defines the volume fraction of the tetrapods and was measured during the

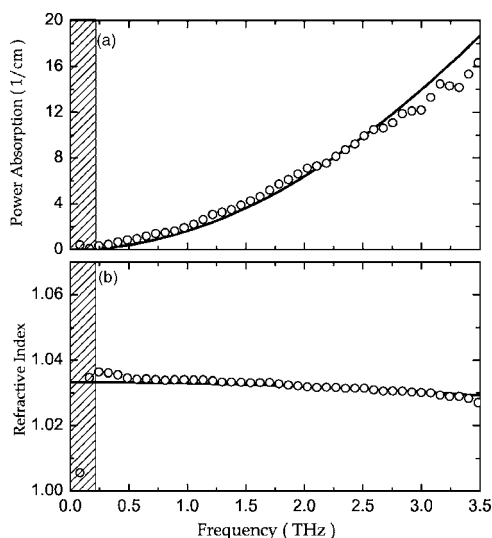


FIG. 2. Comparison of measured results (open circles) with theoretical fitting (solid lines) for the composite ZnO tetrapod samples: (a) power absorption $\alpha(\omega)$; (b) refractive index $n(\omega)$.

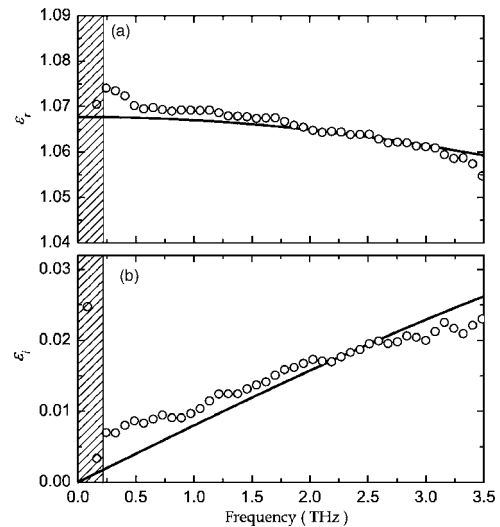


FIG. 3. Frequency-dependent complex dielectric function of the composite ZnO tetrapod samples: (a) real part $\varepsilon_r(\omega)$ and (b) imaginary part $\varepsilon_i(\omega)$. The solid curves and the open circles represent the theoretical fitting and the experimental data, respectively.

experiment, and ε_h and ε_m are the dielectric constants of the host medium and the pure ZnO tetrapods, respectively. In our case, $\varepsilon_h = \varepsilon_{\text{air}} = 1.0$, and the frequency-dependent dielectric function of the pure ZnO tetrapods (a semiconductor) $\varepsilon_m(\omega)$ can be represented by^{18–22}

$$\varepsilon_m(\omega) = \varepsilon_\infty - \frac{\omega_p^2}{\omega^2 + i\gamma\omega} + \sum_j \frac{\varepsilon_{\text{st}j}\omega_{\text{TO}j}^2}{\omega_{\text{TO}j}^2 - \omega^2 - i\Gamma_j\omega}, \quad (1)$$

where ε_∞ is the high-frequency dielectric constant, the second term describes the contribution of free electrons or plasmons, and the third term is due to the contribution of optical phonons. The key parameters describing the dynamics of free electrons or plasmons in a semiconductor are the plasma frequency $\omega_p = (Ne^2/\varepsilon_0 m^*)^{1/2}$ and the carrier damping constant γ , where N is the carrier density, m^* is the effective mass of the electron, and ε_0 is the free-space permittivity (8.854×10^{-12} F/m). The mobility can be obtained from $\mu = e/(m^*\gamma)$. The summation term in Eq. (1) is over all lattice oscillations with the j th transverse optical (TO) frequency $\omega_{\text{TO}j}$, oscillator strength $\varepsilon_{\text{st}j}$, and phonon damping constant Γ_j . For the hexagonal wurtzite bulk ZnO in the terahertz region, it is known that the main dielectric response is from the $E_1(\text{TO})$ vibrational mode.²³ Thus, based on Eq. (1), the dielectric function $\varepsilon(\omega)$ describing our measured sample can be simplified as¹⁹

$$\varepsilon_m(\omega) = \varepsilon_\infty + \frac{\varepsilon_{\text{st}}\omega_{\text{TO}}^2}{\omega_{\text{TO}}^2 - \omega^2 - i\Gamma\omega}. \quad (2)$$

Using Eq. (2), and the simple EMT with $\varepsilon_h = \varepsilon_{\text{air}} = 1.0$, one can achieve a best fit (solid curves in Fig. 3) on the experimental data with the following parameters: $f = 0.01736$, $\varepsilon_\infty = 1.50$, $\varepsilon_{\text{st}} = 3.40$, $\omega_{\text{TO}}/2\pi = 12.41 \pm 0.2$ THz, and $\Gamma/2\pi = 21.0 \pm 0.2$ THz.²⁴ The solid curves shown in Fig. 2 represent the fitting of power absorption and the index of refraction using the same parameters. The fitting reveals the presence of a dominant TO-phonon resonance of ZnO tetrapods, centered at $\omega_{\text{TO}}/2\pi = 12.41$ THz with a phonon damping constant $\Gamma/2\pi = 21.0$ THz and a strength $\varepsilon_{\text{st}} = 3.40$. It is worth noting that such a TO mode at 12.41 THz is a typical transverse optical mode in the bulk ZnO of wurtzite structure

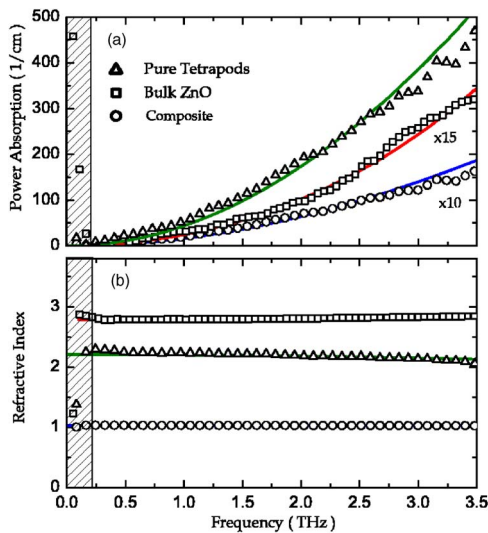


FIG. 4. (Color online) Comparison of (a) measured power absorption and (b) refractive index of the pure ZnO tetrapods (triangles) with that of single-crystal ZnO (squares) and the composite tetrapod samples (circles). The solid curves are the corresponding theoretical fit.

with the assignment $E_1(\text{TO})$.²³ If τ is the TO phonon lifetime, we have $\tau=1/\Gamma$, with value $\tau=7.6$ fs. Actually, τ depends very critically on the type of phonon scattering mechanism, and different scattering laws usually define the various lifetimes. The obtained TO-phonon lifetime τ results mainly from the calculation of absorption, in which scattering from transverse optical phonon has been considered.¹⁹

Figure 4 shows the power absorption and refractive index of the pure ZnO tetrapods, extracted using Eq. (2) and the simple EMT, in comparison with that of the single-crystal ZnO and the tetrapod-air composite sample. The measured single-crystal ZnO is an undoped, high purity (>99.99%), 5 mm \times 5 mm \times 0.5-mm-thick, freestanding slab with wurtzite structure.²⁵ From Fig. 4, it is seen that the terahertz spectra of the single-crystal ZnO exhibit similar behavior as that of the ZnO tetrapod media. The pure ZnO tetrapods represent an obviously higher power absorption than that of the composite tetrapods and the single-crystal ZnO. The refractive index of the pure ZnO tetrapods, 2.21, is close to the value 2.80 of the single-crystal ZnO, but much larger than 1.03, the value for the measured composite tetrapod medium. Based on Eq. (2), the experimental data (squares) of single-crystal ZnO are well fitted using the parameters $\epsilon_\infty=3.705$, $\epsilon_{st}=4.065$, $\omega_{\text{TO}}/2\pi=12.42$ THz, and $\Gamma/2\pi=0.82$ THz. It shows that the terahertz spectrum of the single-crystal ZnO is also dominated by the $E_1(\text{TO})$ phonon mode centered at the frequency of 12.42 THz. All of these features indicate that the ZnO tetrapod structures reveal quite similar phonon response characteristics as the single-crystal ZnO in the low-frequency terahertz regime.

Nanostructures usually present a quite dissimilar optical property from bulk materials due to their high surface-to-volume ratio or their drastic changes in electron structures. Quantum confinement effects are often expected and observed in nanostructures. However, our THz-TDS study has shown that the terahertz spectra of ZnO tetrapods are similar to that of bulk single-crystal ZnO. This implies that the ZnO tetrapods preserve almost the overall crystal structure of the bulk ZnO. This result is also consistent with that of ZnO nanoparticles and ZnO nanotubes.^{26,27} When the radius of the

nanostructures approaches the Bohr radius of exciton, the quantum confinement effect will become noticeable. The diameter of the legs in ZnO tetrapods is between 200 and 800 nm, much larger than the Bohr radius of ZnO (the calculated value is ~ 2 nm). This is why there are no obvious distinctions observed in dielectric properties between the single-crystal ZnO and tetrapod structures.²⁷

The authors acknowledge the fruitful discussions with X. C. Xie. This work was partially supported by the National Science Foundation, the Oklahoma EPSCoR for the National Science Foundation, and the China Scholarship Council. Two of the authors (S.H.L. and Y.P.Z.) were supported by the National Science Foundation under Contract No. ECS-0304340.

¹R. Wu, Y. Yang, S. Cong, Z. Wu, C. Xie, U. Hiroyuki, K. Kawaguchi, and N. Koshizaki, *Chem. Phys. Lett.* **406**, 457 (2005).

²W. Zhang, H. Wang, K. S. Wong, Z. K. Tang, and G. K. L. Wong, *Appl. Phys. Lett.* **75**, 3321 (1999).

³S. Ono, H. Murakami, A. Quema, G. Diwa, N. Sarukura, R. Nagasaka, Y. Ichikawa, E. Oshima, H. Ogino, A. Yoshikawa, and T. Fukuda, *Technical Digest of CLEO' 2005*, 22–27 May 2005, Baltimore, MD (CD ROM), Paper CThX6.

⁴Z. R. Tian, J. A. Voigt, J. Liu, B. Mckenzie, M. J. McDermott, M. A. Rodriguez, H. Kngishi, and H. Xu, *Nat. Mater.* **2**, 821 (2003).

⁵V. A. L. Roy, A. B. Djuricic, W. K. Chan, J. Gao, H. F. Lui, and C. Surya, *Appl. Phys. Lett.* **83**, 141 (2003).

⁶R. Wu, J. Wu, C. Xie, X. Zhang, and A. Wang, *Mater. Sci. Eng., A* **328**, 196 (2002).

⁷X. Chu, D. Jiang, B. A. Djuricic, and H. Y. Leung, *Chem. Phys. Lett.* **401**, 426 (2005).

⁸V. A. L. Roy, A. B. Djuricic, H. Liu, X. X. Zhang, Y. H. Leung, M. H. Xie, J. Gao, H. F. Lui, and C. Surya, *Appl. Phys. Lett.* **84**, 756 (2004).

⁹J. K. Song, J. M. Szarko, S. R. Leone, S. Li, and Y. Zhao, *J. Phys. Chem. B* **109**, 15749 (2005).

¹⁰J. M. Szarko, J. K. Song, C. W. Blackledge, I. Swart, S. R. Leone, S.-H. Li, and Y.-P. Zhao, *Chem. Phys. Lett.* **404**, 171 (2005).

¹¹D. Grischkowsky, S. Keiding, M. van Exter, and Ch. Fattinger, *J. Opt. Soc. Am. B* **7**, 2006 (1990).

¹²H.-Ch. Weissker, J. Furthmuller, and F. Bechstedt, *Phys. Rev. B* **67**, 165322 (2003).

¹³S. Fratini, F. de Pasquale, and S. Ciuchi, *Phys. Rev. B* **63**, 153101 (2001).

¹⁴L. Thamizhmani, A. K. Azad, J. Dai, and W. Zhang, *Appl. Phys. Lett.* **86**, 131111 (2005).

¹⁵Z. Chen, Z. Shan, M. S. Cao, L. Lu, and S. X. Mao, *Nanotechnology* **15**, 365 (2004).

¹⁶Y. H. Leung, A. B. Djuricic, J. Gao, M. H. Xie, and W. K. Chan, *Chem. Phys. Lett.* **385**, 155 (2004).

¹⁷W. Zhang, A. K. Azad, and D. Grischkowsky, *Appl. Phys. Lett.* **82**, 2841 (2003).

¹⁸M. Grynberg, R. Le Toullec, and M. Balkanski, *Phys. Rev. B* **9**, 517 (1974).

¹⁹M. Balkanski, in *Optical Properties of Solids*, edited by F. Abelès (North-Holland, New York, 1972), Chap. 8.

²⁰J. Han, F. Wan, Z. Zhu, Y. Liao, T. Ji, M. Ge, and Z. Zhang, *Appl. Phys. Lett.* **87**, 172107 (2005).

²¹J. Han, W. Zhang, W. Chen, L. Thamizhmani, A. K. Azad, and Z. Zhu, *J. Phys. Chem. B* **110**, 1989 (2006).

²²B. L. Yu, F. Zeng, V. Kartazayev, R. R. Alfano, and K. C. Mandal, *Appl. Phys. Lett.* **87**, 182104 (2005).

²³C. A. Arguello, D. L. Rousseau, and S. P. S. Porto, *Phys. Rev.* **181**, 1351 (1969).

²⁴*Physics of II-VI and I-VII Compounds; Semimagnetic Semiconductors*, edited by O. Madelung (Springer, Berlin, 1982), Chap. 3.

²⁵A. K. Azad, J. G. Han, and W. Zhang, *Appl. Phys. Lett.* **88**, 021103 (2006).

²⁶M. Rajalakshmi, A. K. Arora, B. S. Bendre, and S. Mahamuni, *J. Appl. Phys.* **87**, 2445 (2000).

²⁷Y. J. Xing, Z. H. Xi, Z. Q. Xue, X. D. Zhang, J. H. Song, R. M. Wang, J. Xu, Y. Song, S. L. Zhang, and D. P. Yu, *Appl. Phys. Lett.* **83**, 1689 (2003).